Check for updates

# Nanoparticle-Mediated Photoporation: Expanding Horizons in Drug Delivery

Erin McGraw,[a] Guillaume M. Laurent[b] and L. Adriana Avila [ID] *[a]

Facilitating the delivery of impermeable molecules into cells stands as a pivotal step for both basic research and therapeutic delivery. While current methods predominantly use nanoparticles or viral vectors, the exploration of physical phenomena, particularly light-based techniques, remains relatively under-explored. Photoporation, a physical method, employs either pulsed or continuous wave lasers to create transient pores in cell membranes. These openings enable the entry of exogenous, membrane-impermeable molecules into the cytosol while preserving cell viability. Poration can either be achieved directly through focusing a laser beam onto a cell membrane, or indirectly through the addition of sensitizing nanoparticles that interact with the laser pulses. Nanoparticle-mediated photoporation specifically has recently been receiving increasing attention for the high-throughput ability to transfect cells, which also has exciting potential for clinical translation. Here, we begin with a snapshot of the current state of direct and indirect photoporation and the mechanisms that contribute to cell pore formation and molecule delivery. Following this, we present an outline of the evolution of photoporation methodologies for mammalian and non-mammalian cells, accompanied by a description of variations in experimental setups among photoporation systems. Finally, we discuss the potential clinical translation of photoporation and offer our perspective on recent key findings in the field, addressing unmet needs, gaps, and inconsistencies.

[a]Department of Biological Sciences, Auburn University, Auburn, AL 36849, USA. E-mail: adriana.avila@auburn.edu; Tel: +1-334-844-1639

[b]Department of Physics, Auburn University, Auburn, AL 36849, USA

## 1    Introduction

The delivery of exogenous biological molecules (*e.g.*, RNAs, plasmids, and proteins) into cells is a crucial part of not only fundamental cell-based research, but also for the development

*Erin McGraw is a fifth year PhD candidate at Auburn University, Auburn, Alabama, under the supervision of Dr Adriana Avila. Her dissertation topic focuses on the development and optimization of nanoparticle-based nucleic acid delivery methods, such as photoporation. Additionally, she studies the potential of bio-derived, peptide-based nanoparticles as an insect pest control alternative.*

**Erin McGraw**

*She received her BSc in Biochemistry from Auburn University in 2019, during which she studied the effects of tau protein accumulation in rodent models of Alzheimer's disease. Her academic interests include exploring nucleic acid-based therapies against pathogens and pests, and her personal interests include crocheting and reading.*

*Guillaume. M. Laurent is a Full professor in the Physics Department at Auburn University and the Head of the Auburn Source of Attosecond Pulses (ASAP) laboratory. He received his PhD in 2004 from the University of Caen (France) and later on worked at the Universidad Autonoma de Madrid (Spain), Kansas State University, and at MIT as a postdoctoral fellow and research scientist. His current research interests*

**Guillaume M. Laurent**

*include time-resolved measurements at the attosecond timescale, the development of novel sources of attosecond pulses, the fabrication of thin-film semiconductors, and the laser-induced delivery in biological systems.*

of new therapies, biological imaging techniques, and drug delivery systems. An important challenge in delivering clinical molecules is crossing the cell membrane, a highly selective physical and chemical barrier that is difficult to bypass. Broadly speaking, delivery methods capable of traversing the cell membrane can be classified as chemical, biological, or physical. Chemical transfection reagents, such as calcium chloride and cationic polymers, take advantage of electrochemical interactions of ions or cargo with the negatively charged cell membrane. Chemical methods are generally the most simple and accessible for many applications. However, these methods are limited by factors such as stability in blood/serum, toxicity, and challenges related to solubility.[1]

Viruses are a prime example of naturally occurring biological delivery systems capable of crossing cellular barriers to deliver nucleic acids into the cytosol. Viruses such as baculovirus and adeno-associated viruses (AAVs) can be genetically modified to deliver therapeutic nucleic acids to specific cells types *in vivo*.[2] However, AAVs also possess the ability to incite immune responses, which can potentially diminish or negate the desired therapeutic effects. Additionally, other risks such as insertional mutagenesis have also limited their use in a clinical setting, thus novel non-viral delivery methods are in demand for high-throughput gene delivery.

Common physical delivery methods are able to utilize physical phenomena such as force, electricity, or other energy-dependent methods to target either single cells, such as single-cell injections, or multi-cell delivery. While single cell injections also result in high success rates, it generally requires specialized equipment and highly trained personnel. Additionally, delivery into individual cells in incredibly time consuming and is a notable limitation of the technique. Delivery into solutions with high cell concentrations generally requires the use of higher-intensity forces which may damage cells or cargo. Thus, while physical strategies, such as biolistic, sonoporation, heat shock, and electroporation, offer simpler

methodologies, the use of strong physical forces may compromise nucleic acid integrity or result in increased cell mortality.[1]

Photoporation, a technique enabling the introduction of membrane-impermeable molecules into cells using continuous or pulsed laser light, is emerging as an exciting physical delivery method. Since its introduction, photoporation has evolved dramatically, thanks to the implementation of ultra-fast pulsed-laser systems. Ultra-fast lasers deliver sub-nanosecond light pulses with extremely high peak intensities that easily exceed several tens of PW cm$^{-2}$ (1 PW = $10^{15}$ W) and extremely short pulse durations, up to the femtosecond (1 fs = $10^{-15}$ s) regime. In virtue of these unique properties, such laser systems are most frequently used for photoporation. Unlike ultra-fast irradiation, use of nanosecond pulses results in intense photothermal heating of the irradiated solution that may compromise membrane integrity and viability, while irradiation with ultra-fast lasers avoids heating due to the previously mentioned extremely short pulse duration and subsequent "dark time". Additionally, ultra-fast pulses reduce the laser-induced breakdown (LIB) threshold of molecules, which, as we will explain in detail later, results in the generation of solvated electrons that form localized, low-density plasmas that contribute to additional photochemical and photophysical processes. Thus, femtosecond lasers are generally more suitable for delivery of molecules into cells due to this gentler approach.[3,4]

Publications reporting delivery *via* photoporation are still scarce compared to the literature focusing on other physical delivery methods such as electroporation, biolistics, microinjection, and sonoporation. As of writing, a keyword search of PubMed and Google Scholar resulted in 67 and 1200 results for "photoporation" over the last ∼25 years (since 2000), respectively (Table 1), while more common, clinically proven chemical reagents, such as "lipid nanoparticles" returned 7569 and 18 100 search results. Physical systems rely on the use of physical phenomena such as electricity, heat, or mechanical force (*e.g.*, cavitation) to weaken the cell membrane. While physical methods are some of the oldest bench top delivery methods, they have not maintained the same level of clinical translation as chemical or biological-based delivery methods, likely due to

*L. Adriana Avila is currently an Associate Professor and an Undergraduate Program Officer in Auburn University Department of Biological Sciences. Her research focuses on innovative delivery platforms for nucleic acids. She earned an MS in Organic Chemistry from the University of the Basque Country, Bilbao, Spain, and gained industry experience for two years at a Biotechnology Company. Later, she completed her PhD in Biochemistry and Molecular Biophysics at Kansas State University in 2010, followed by postdoctoral research at Kansas State University and Auburn University. She began her tenure-track position in Biological Sciences at Auburn University in 2017.*

**L. Adriana Avila**

**Table 1** Keyword search for common delivery methods from 2000 to the present using PubMed and Google Scholar, the two commonly used scientific search engines

| Keyword | PubMed | Google Scholar |
| --- | --- | --- |
| Intracellular physical delivery methods | 678 | 104 000 |
| Intracellular chemical delivery methods | 2373 | 49 600 |
| Intracellular biological delivery methods | 5373 | 61 700 |
| Nanoparticle delivery system | 48 262 | 18 300 |
| Photoporation | 67 | 1200 |
| Optical transfection | 5249 | 103 000 |
| Photothermal therapy | 11 615 | 230 000 |
| Electroporation | 15 080 | 258 000 |
| Adenovirus vector | 16 726 | 18 600 |
| Lipid nanoparticles | 7569 | 18 100 |
| Liposomes | 59 494 | 191 000 |
| Lipofectamine | 3441 | 71 800 |
| Calcium phosphate transfection | 549 | 23 100 |

some inherent barriers associated with using physical forces. For example, biological and chemical methods can be finely tuned to target specific organs, tissues, or cell types, while physical methods are more broadly focused and less targetable. Despite this, physical methods can be applied to nearly all cell types (mammalian, fungi, algae, *etc.*) and hold the potential for incredibly high throughput, thus making them promising for both laboratory and clinical studies.

Photoporation has been demonstrated in a variety of cell types to deliver several different molecules (*e.g.*, reporter dyes, nucleic acids, and proteins), and thus has potential in many different therapies.[5–7] For example, Batabyal *et al.* reported the successful *in vitro* and *in vivo* delivery of opsin-encoding genes using pulsed fs laser light.[8] Additionally, the development of this technique will provide an alternative drug delivery tool for infections that are resistant to current chemical and biological treatments as cells cannot develop resistance against physical phenomena (*e.g.*, lasers, electricity, heat, *etc.*) as they do for chemical compounds.

Although less understood, compared to other physical methods such as electroporation, photoporation holds significant promise for nucleic acid delivery. This potential stems from the distinctive lasers utilized, the absence of cellular resistance to this particular physical phenomenon, and the temporary nature of the pores formed in cells during irradiation. Nonetheless, conditions for optimal delivery remain uncertain as they depend heavily on a complex network of variables, including if the laser source is continuous or pulsed, light wavelength, laser power, and irradiation time. This review will first briefly discuss the specific mechanisms behind photoporation and provide a snapshot of the current state of this technology, including the recent understanding of laser–nanoparticle interactions, the use of different nanoparticles, and the implications of current *in vitro* delivery in various cell types. Additionally, the use of photoporation for delivery in non-mammalian cells will be discussed. Lastly, the authors will give a brief overview of the potential implications for the clinical application of photoporation and unmet needs in this regard.

## 2 Recent contributions to the understanding of photoporation mechanisms

Photoporation can occur *via* direct interactions between the laser and cell membrane or indirectly through nanoparticle-mediated processes. In direct photoporation, the laser must be focused individually on each cell with high spatial and temporal precision in order for enough energy to be delivered for pore formation in the cell membrane (Fig. 1A).[9,10] Additionally, effects of different laser types, irradiation conditions, cell viability, comparative delivery efficiency, and bioeffects resulting from irradiation are not usually reported. For example, one of the few publications that successfully demonstrated the use of a commonly available, continuous-wave laser to achieve successful transfection was published by Paterson *et al.* in 2005.[9] In this work, the group delivered pDNA encoding
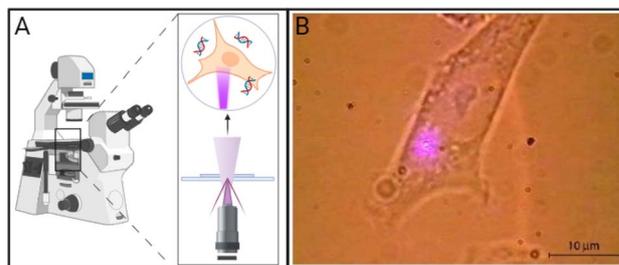


Fig. 1 (A) Schematic of direct photoporation in which lasers must generally be tightly focused on the surface of the cell, generally through an inverted or a confocal microscope. (B) Micrograph of a CHO-K1 cell exposed to a 405 nm violet diode laser focused through a 100× objective of an inverted microscope resulting in direct photoporation. Adapted with permission from ref. 9 © The Optical Society. Created using https://BioRender.com.

for antibiotic resistance and GFP using a 405 nm violet diode laser focused through a 100× objective onto CHO-K1 cell membranes (Fig. 1B).[9] Although the authors reported 100% poration, no data on other relevant bioeffects, such as toxicity or production of reactive species, were reported. Additionally, Batabyal *et al.* reported one of the only clinically relevant examples of direct photoporation to date. *In vitro* and *in vivo* delivery of pDNA using a 1030 nm laser with a 100 fs pulse duration focused through a 10× objective of an Olympus fluorescence microscope resulted in minimum damage and reliable expression of multicharacteristic opsin and mCherry fluorescent protein in opsin-sensitized retinal cells.[8] Excitingly, both fluorescence imaging of mCherry and *in vivo* electrical recordings showed the functionality of the retinal cells. However, this study only reported viability based on caspase activity and did not discuss other relevant bioeffects. The lack of reported biologically relevant data, the higher energy lasers that may damage cells or cargo, and the time-consuming systematic irradiation of each individual cell are all factors that contribute to the lack of advancement in direct photoporation.

In contrast, the addition of nanoparticles enables the use of ultra-fast lasers which deliver less energy per unit of time, which ultimately preserves viability. The delivered energy is able to transform from interactions with the nanoparticles into chemical (electron cascades) and physical (photoacoustic waves, cavitation) energy, which has a prolonged effect within the system.[11–13] This enables nanoparticle-mediated systems to have higher throughput, where cultures of cells may be scanned rapidly with a laser, or cells may be suspended in solution and irradiated with a stationary laser.[6,14,15]

A wide variety of nanoparticles have been used in photoporation systems, including carbon black, gold, various metal oxides, and quantum dots.[16–18] When added to photoporation samples, recent findings have demonstrated that they enhance the effects caused by the laser by interacting with the electromagnetic field of the pulse, ultimately leading to increased pore formation and cargo delivery. Additionally, the pairing of different lasers with different nanoparticles can drastically affect the delivery rates of a system, such as in the case of gold,

a highly photo-responsive material that behaves differently depending on the laser light it is exposed to.

One of the most understood mechanisms is the formation of vapor nanobubbles around nanoparticles that then rapidly collapse and release acoustic waves and a stream of air, a process known as cavitation.[19,20] This effect can be compounding, as the pressure imbalance resulting from the imploding bubble can trigger a cascade of cavitation events until the energy is able to dissipate throughout the surrounding media.[11] Other effects include the LIB of water, in which solvated electrons resulting from the generation of hydroxyl radicals, according to $H_2O + h\nu \rightarrow {}^{\cdot}OH + H^+ + e^-(aq)$, are cascaded into solution, forming a localized plasma that contributes to further cavitation events. Vogel *et al.* explored the temperature distribution of photoporation samples irradiated with either continuous wave lasers or femtosecond-pulsed lasers and showed that in the case of fs-pules, the generated free electron distribution increases the spatial resolution, and thus the accuracy, of fs laser systems.[21] Similarly, surface plasmon resonance (SPR), or the formation of an energy-dense plasma around laser-activated nanoparticles, is frequently observed with metallic nanoparticles that have an absorbance wavelength same as the irradiation wavelength.[17,21,22] In the following sections, we will provide more details about the mechanisms underlying nanoparticle-mediated photoporation.

## 2.1 Indirect photoporation

Most examples of photoporation utilize some type of sensitizing nanoparticle that interacts with the laser energy. Nanoparticle-mediated photoporation occurs *via* indirect effects that result from interactions between the laser light and nanoparticles. These effects can be classified as in-resonance or off-resonance depending on how the nanoparticles interact with the electromagnetic energy of the laser. In-resonance interactions require the nanoparticle absorbance wavelength to be the same as the wavelength of the laser.[17] This causes the nanoparticle to absorb the pulsed laser energy, resulting in a phenomenon known as surface plasmon resonance (SPR). Alternatively, off-resonance interactions occur when the absorbance wavelength of the nanoparticle and the wavelength of the laser are different. These effects, which are generally less intense, include cavitation, laser-induced solution breakdown, and temporary localized heating. Off-resonance effects greatly depend on factors such as nanoparticle size and concentration. Both mechanisms, off- and in-resonance will be further discussed in the following section. However, before expanding our discussion on mechanisms it is necessary to bring to attention the lack of research on the impact of nanoparticle surface functionalization on delivery efficacy. While it is well documented that these modifications play significant roles in colloidal stability and cell membrane affinity, studies directly comparing surface modifications of the same particle type are rare.[18,23,24] Additionally, variations in nanoparticle–laser interaction underscore the importance of both the laser wavelength and nanoparticle absorbance wavelength in the development of a photoporation system. For example, one exciting aspect of gold nanoparticles and

quantum dots is their ability to adjust the maximum absorbance wavelength using particle size and shape. This enables the system to be either off- or in-resonance while still utilizing the same type of particle, a fact that is discussed more in-depth in Section 2.2.1.

In many instances, cells are first incubated with nanoparticles prior to irradiation to allow the nanoparticles to settle onto the cell surface; however, nanoparticles may also be left suspended in solution.[15,23,25] While gold nanoparticles (AuNPs) are most commonly used due to their unique energy-absorbing properties, a variety of other nanoparticles such as carbon-based nanoparticles, quantum dots, and others have been reported for both methods. Nanoparticle-mediated photoporation has become more common than direct photoporation, likely due to the versatility provided by the nanoparticles. For example, the choice of in-resonance or off-resonance may greatly impact the dominant effects that occur during photoporation. Additionally, nanoparticle size, material, or surface modification may also be selected to specifically complement the goal of photoporation (*e.g.*, delivery of nucleic acids *vs.* microscopic studies of the cell membrane).

### 2.1.1 Laser–nanoparticle interactions

*Off-resonance effects.* Off-resonance effects occur when the absorbance wavelength range of the nanoparticle is different from that of the wavelength of pulsed photons. These effects generally include those presented in Fig. 2A–C.

● Localized surface heating[12,19,26] – as the nanoparticle is subjected to ultra-fast laser pulses, a plasma forms near the surface of the nanoparticle from the interactions of the incident electromagnetic waves and the nanoparticle's surface electrons. In the case of AuNPs, collisions between electrons in the plasma and water molecules cause a variety of cascading thermoemission effects. These effects occur in picoseconds prior to cavitation and will build if energy is not dissipated, which may happen if low laser intensities are used and cavitation is not triggered (Fig. 2A).

● Laser-induced breakdown[11,12,27] – the energy threshold at which a solution heats to ionization temperatures, resulting in the formation of a plasma filled with solvated electrons. This process generates a shock wave that propagates through the surrounding liquid (Fig. 2B).

● Cavitation[11,12,28] – following LIB, a vapor nanobubble is left in the void from the propagating shock wave. The bubble will increase in size according to the energy of the shock wave, followed by a rapid implosion which releases another shock wave and a jet of air. This effect cascades until the energy is dissipated through factors such as cooling, solution viscosity, and others. Boulais *et al.* showed that at higher laser intensities, off-resonance nanoparticles triggered cavitation but did not result in nanoparticle fragmentation[12] (Fig. 2C).

The specifics of these effects (duration, intensity, nanobubble size, *etc.*) depend on the specifics on the unique combination of laser-specific conditions (pulse duration, total irradiation time, *etc.*) and nanoparticle-specific conditions (concentration, shape, size, *etc.*). This multi-faceted interaction of variables is one of the clear challenges in directly comparing different systems. For example, even slight variations in nanoparticle size can significantly alter how the nanoparticle absorbs
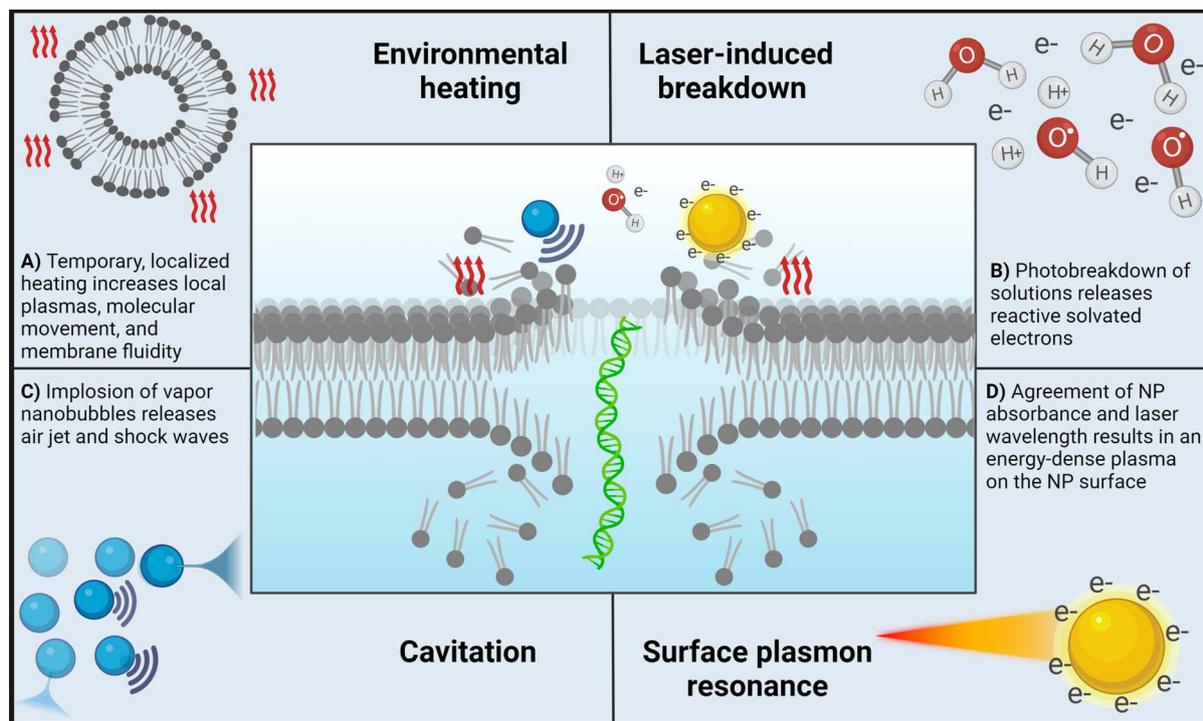
**Fig. 2** Schematic representing the different effects resulting from off-resonance (A–C) or in-resonance (D) interactions. (A) The "off" time between laser pulses allows localized heat to quickly dissipate, thus increasing membrane permeability while preventing heat damage to cells. (B) The molecular breakdown of the solution releases high-energy electrons into solution that contribute to other energetic phenomena. (C) The implosion of vapor nanobubbles releases a jet of air and photoacoustic waves that concuss the cell membrane. (D) When a nanoparticle is able to absorb energy at the same wavelength as the emitted laser pulse, an energy-dense plasma forms on the nanoparticle surface. This plasma cascades electrons into solution and enhances other effects, similar to LIB. Created with https://BioRender.com.

and scatters light, interacts with cells, and may even exhibit toxic effects.[29,30]

*In-resonance effects.* In-resonance effects occur when the wavelength of the pulsed photons is the same as the absorbance wavelength of the nanoparticle.[31] The effects seen in resonant systems encompass more intense instances of the off-resonance phenomena, as well as the following:

• Surface plasmon resonance (SPR):[12,13,17] similar to how a photon is a quantization of light, plasmons are quantizations of collective plasmon oscillations, or oscillations in the electron 'fluid' surrounding some nanoparticles such as AuNPs. Due to the incredibly small size, plasmon excitement by the electromagnetic field of a laser pulse creates a localized plasma through the whole nanoparticle volume. This results in a highly intense energetic phenomenon near the nanoparticle surface that can be nearly eleven times stronger than that in the off-resonance cases[12] (Fig. 2D).

SPR stands out as one of the most frequently documented in-resonance phenomena. It is essential to note that extreme heating has the potential to induce nanoparticle damage, which, in turn, may result in unintended harm to cells or adjacent tissues.[27]

## 2.2 Laser-activated nanoparticles: specific examples

In addition to the optimization of laser parameters, the incorporation of nanoparticles into a photoporation system presents another exciting area of customizability. Variables such as material, size, shape, surface functionalization, and absorbance spectra all play a role in the overall delivery efficacy.[10,16,17] The following section highlights a set of nanoparticle-mediated systems to showcase the variability that these conditions have on overall delivery efficacy, and a summary can be found in Table 2.

**2.2.1 Gold nanoparticles.** AuNPs are the most commonly used nanoparticles in photoporation methods for several reasons. First, they are readily available from commercial manufacturers or can be easily synthesized. Additionally, the nanoparticle surface can be functionalized with a wide variety of molecules such as PEG, oligonucleotides, biotin, and more. Lastly, AuNPs can be in- or off-resonance with the laser in use, as mentioned previously. AuNPs may be easily synthesized in a variety of shapes and sizes, which impacts the maximum absorbance wavelength and various light-scattering properties of the particle.[42] For example, a 10 nm AuNP has a $\lambda_{max}$ of ~520 nm, while a 40 nm particle has a $\lambda_{max}$ of ~530 nm. Thus, tuning these characteristics makes it possible to customize a particle to create an in- or off-resonance system, a key feature in the popularity of AuNPs. This distinction has major implications for the underlying mechanisms responsible for membrane permeabilization.

As mentioned previously, off-resonance effects occur when the absorbance wavelength of the AuNP is not equal to the wavelength of the irradiating laser. Effects that result from this

Table 2  Summary of highlighted examples of molecule delivery in mammalian cells *via* nanoparticle-mediated photoporation

| Nanoparticle | Cell type | Cargo | Hypothesized mechanism | Ref. |
|---|---|---|---|---|
| **In-resonance** | | | | |
| Gold nanoparticles | | | | |
| Nanospheres | HN31, T-cells, and Jurkat | FITC–dextran and pDNA | Plasmonic nanobubbles | 32 and 33 |
| | Hodgkin's L428 and Karpas 299 | Various antibodies | Localized heating, cavitation, and propagating stress waves | 34 |
| Pyramid array | Myoblast C2C12 | Calcein | Various plasmonic effects | 14 |
| **Off-resonance** | | | | |
| Gold nanoparticles | | | | |
| Nanospheres | CHO | Calcein and pDNA | Cavitation and laser-induced breakdown | 15 |
| | HeLa and H1299-EGFP | Calcein, FITC–dextran, and siRNA | Vapor nanobubbles and AuNP heating | 19 |
| Quantum dots | | | | |
| Graphene QDs | HeLa | FITC–dextran | Vapor nanobubbles | 35 |
| Black phosphorus QDs | HeLa | siRNA and mRNA | Vapor nanobubbles | 26 and 36 |
| Carbon-based | | | | |
| Carbon black | DU145 and GS-9L | Calcein, BSA, and pDNA | Photoacoustic bubble formation and shock wave propagation | 5 and 37 |
| | DU145 and H9c2 | Calcein and FITC–dextran | Photoacoustic effects | 38 |
| Carbon nanotubes | DU145 | Calcein | Vapor nanobubble formation and localized temporary heating | 37 and 39 |
| Metal oxides | | | | |
| Iron oxide | Embryonic stem cells and T-cells | siRNA, FITC–dextran, and CRISPR–Cas9 RNP | Photothermal effects from nanoparticle proximity and ns-pulse effects | 40 |
| Titanium oxide | HeLa | Calcein, propidium iodide, and TRITC–dextran | Combination of photochemical, nanobubbles, and localized heating | 41 |

interaction are generally less localized and thus may result in lower delivery rates.[12] However, systems using more delicate cells may benefit from this as these less-intense effects have less impact on cell viability. For example, McGraw *et al.* delivered the reporter dye calcein into CHO cells.[15] In this study, CHO cells were used to understand how irradiation conditions required to deliver molecules into more resilient fungal cells may impact mammalian cells. While delivery of calcein into CHO cells was possible at much lower laser powers and irradiation times, viability of CHO cells suffered due to the increased laser intensity needed to deliver molecules into the fungal cells.[15]

Gold nanoparticles that have a plasmonic resonance that is in tune with the laser being used trigger in-resonance effects.[14,19,23,32–34,43] In-resonance AuNPs absorb laser light, resulting in localized heating and the production of vapor nanobubbles that have been used to deliver a variety of molecules such as fluorescent dyes, plasmids, proteins, and even bacteria. Saklayen *et al.* were able to quantify changes in the plasma membrane resulting from in-resonance effects.[14] Of note, they were able to deliver the fluorescent reporter dye calcein AM with 80% efficiency and maintaining ∼90% viability. Their setup utilized an array of 50 nm Au nanopyramids laid on a glass slide that were irradiated with a scanning laser beam. Localized effects due to the in-resonance particles resulted in enhanced delivery with non-impacted viability.

While the enhanced effects of SPR may seem desirable, as mentioned above, the intense energy the nanoparticles are subjected to may result in fragmentation. At laser fluences around 2 mJ cm$^{-2}$, gold nanorods have been imaged fragmenting into smaller rods or spheres.[44] While this is a useful tool for synthesis and shaping of AuNP colloids, it could present a risk for clinical translation of this technology. This is yet another area of potential research needed to understand how the complex web of variables involved in this system are related to each other and need to be optimized.

**2.2.2 Quantum dots.** Quantum dots (QDs) are semiconductor nanoparticles that have unique optical and electronic properties. Due to their incredibly small size (1–10 nm), the sub-atomic (quantum) interactions resulting from the discretization of energy levels within the semi-conductive metal core are intense enough to be impactful in the system. QDs can be made of a variety of materials but are generally binary metal compounds from groups II–VI of the periodic table or materials from groups III–V that are coated with ZnS. Additionally, these particles may be coated with stabilizing materials such as silica or contain other surface modifications. One attractive feature of QDs is the tunability of their absorbance and emission spectra, which is most clearly seen in metals such as gold, where even single nm changes in size can noticeably shift the absorbance spectra until around ∼10 nm in size.[45] This tunability gives QDs the exciting feature of being able to be off- or in-resonance, as

just discussed in the Gold nanoparticles section, while also having the unique feature of being at the lowest limits of the nanoscale. This makes QDs a useful tool for intracellular delivery, tagging, and tracking, and thus delivering QDs *via* photoporation has been more studied than utilizing them as mediators in the process.

Recently, Cd-free and non-metal QDs have shown potential in bioimaging and cell-labeling techniques as they overcome cytotoxicity generally associated with the transition metals commonly found in well-developed QDs such as Cd, Te, Se, and others.[46] Specifically, Liu *et al.* have been one of the only groups to irradiate graphene QDs (GQDs) to deliver a variety of molecules.[35] Their method consists of a "homemade setup" in which HeLa cells grown in glass culture plates were irradiated using a 7 ns pulse of an Opolette™ laser tuned to 561 nm and focused through a 10× objective. Along with molecule delivery, the optical setup allowed for the analysis of energy thresholds required for vapor nanobubble generation of both GQDs and AuNPs. Specifically, the authors point out that GQDs are incredibly thermally stable and thus are more resilient to intense energy of ns pulses compared to gold AuNPs that fragment under such conditions. Delivery rates of FITC–dextran (FD) molecules of varied sizes resulted in up to 51.2% delivery for FD10 (~4 nm) and as low as 18.4% for FD500 (~31 nm), with viability maintained at >80%. Additionally, the exploration of surface modification of these GQDs with polyethylene glycol (PEG) and polyethyleneimine resulted in significantly enhanced colloidal stability and delivery rates (81% for GQD–PEG), thus enforcing the evidence of surface modifications also playing an important role in nanoparticle consideration. Wang *et al.* explored the use of black phosphorus QDs (BPQDs). Their highly tunable size and broad spectrum absorbance make them unique as photoporation sensitizers in that they have successfully been able to deliver mRNA (0.4 μg mL$^{-1}$) into HeLa cells using both 532 nm visible light and 800 nm NIR light, ultimately achieving up to ~53% delivery efficiency.[26,36]

Other forms of QDs have not yet been explored as tools in nanoparticle-mediated photoporation, despite their success in similar systems. Further exploration of QDs could potentially open a new path of combinatorial methods in which QDs are used as both a delivery tool and an intracellular tag.

**2.2.3 Carbon-based nanoparticles.** One unique off-resonance system was reported by the Prausnitz group first in 2010 with the use of carbon black (CB) nanoparticles.[5,38] They reported that unlike the theorized thermal effects resulting from irradiation with AuNPs, the main mechanism responsible may be due to cavitation resulting from the interaction of carbon and steam: $Cs + H_2O \rightarrow CO(g) + H_2(g)$; however, it was determined that photoacoustic effects and the resulting shock wave propagation were the main mechanisms of delivery. Carbon nanotubes (CNTs) have also been reported to interact similarly with laser light, resulting in localized photothermal effects that may be responsible for photoporation; however, no exact mechanisms have been reported for this system.[39,47] Additionally, it has also been demonstrated in DU145 prostate cancer cells that the observed bioeffects post-photoporation change depending on the selection of carbon-based

nanoparticles (multi-walled CNTs, single-walled CNTs, or CB nanoparticles), and it is unlikely that differences are a result of variances in photoacoustic pressures resulting from cavitation events.[37] This presents an interesting path of research for non-metallic nanoparticle-mediated photoporation.

**2.2.4 Metal oxide nanoparticles.** One of the most common metal oxides used in photoporation systems is iron oxide due to their safety (clinically approved MRI contrast agent), magnetic properties, and cellular biodegradability.[26] One exciting example of the use of iron oxide nanoparticles (IONPs) was demonstrated by Xiong *et al.* in their use of IONPs encased in photothermal electrospun nanofibers.[40] This unique approach allowed for the delivery of several molecules, including siRNAs (70–80% efficiency), 10 kDA FITC–dextran (~80% efficiency), and Crisper–Cas9 ribonuclear protein (RNP) complexes (>60% efficiency). It's essential to note that this study utilized a single 7 ns pulse of an Opolette HE 355 LD laser tuned to 647 nm. As previously discussed, the extra energy delivered through a ns-scale pulse has the potential to greatly impact viability. However, the suspension of the IONPs in the nanofibers created an environment such that high delivery rates could be achieved without the expected loss in viability.

While iron oxide is the most common metal oxide used in photoporation systems, it is also possible for other metals to be used. Mohan *et al.* developed and characterized a method utilizing titanium oxide nanospikes. Similar to the previously discussed study, this design also utilized a nanosecond pulse, a feature seemingly consistent in studies utilizing metal oxides. A 5 ns pulse of a 532 nm Cobolt Tor XS laser was used to deliver dyes such as PI and calcein AM and 10 kDa TRITC–dextran into HeLa cells, ultimately achieving ~80–90% efficiency.[41]

### 2.3 Membrane healing post-irradiation

It has been documented that cell membrane repair mechanisms rely on the presence of intracellular Ca$^{2+}$ at the injury site. However, the specific mechanisms and the timing of pore resealing seem to be largely dependent on pore size. Small wounds of only a few nm have been reported to seal spontaneously, while larger micron-sized injuries trigger the recruitment of proteins that will then trigger mechanisms such as pore clogging, membrane shedding, endocytosis, or exocytosis, depending on the wound specifics.[48,49] Pores resulting from laser irradiation are generally in the <100 nm range, so this review will not cover the driving factors in larger (micron-scale) wound healing, but several reviews exist on the topic.[49–51]

Literature exploring the pore healing process post-photoporation is sparse. However, electroporation has been documented to create pores of similar size in yeast, and barrier resealing has been found to take anywhere from 50 ms to 2 s for an initial decrease in pore size, while full resealing may occur gradually over several minutes.[48] Interestingly, it has been documented that pore healing in Ca$^{2+}$-deficient media takes longer compared to media with Ca$^{2+}$, suggesting that the mechanisms of even these small wounds are calcium-dependent.

Documentation of pore healing for photoporation seems to report similar timing. For example, both Kalies *et al.* and

Palankar *et al.* reported the sealing of nm-scale holes to take anywhere from 2 to tens of seconds, while μm-sized holes resulted in cell death.[52,53] Presumably, $Ca^{2+}$ is also needed post-photoporation for cell membrane repair. However, no experimental data are currently available to corroborate this. The cell's capability to heal photoporation-induced wounds is significantly reliant on several factors, including nanoparticle aggregation, concentration, and size. Increases in any of these factors led to elevated levels of cell death. This underscores the critical significance of optimizing nanoparticle parameters in the experimental design of photoporation systems and emphasizes the need for a more systematic comparison of nanoparticle materials and an exploration of how various cell types respond to photoporation. Additionally, no experiments have been conducted in the absence of calcium, thus the role of this ion in membrane healing after photoporation remains unknown, and further study is needed in order to gain a deeper understanding of the impact of such energy-dense reactions on cells.

# 3 Photoporation in non-mammalian cells

While the majority of studies on molecule delivery through photoporation have focused on mammalian systems, a limited number of reports have explored alternative cell types. Of particular significance is the investigation of drug and nucleic acid delivery in diverse organisms, including fungi and bacteria. Such research holds the promise of unlocking novel therapeutic approaches against highly resilient pathogens. Similarly, delivery into plant cells is essential for the development of new molecular breeding techniques needed for the continued advancement of plant genomics. Despite these clear advantages, delivery in these cell types has been limited due to an extra barrier that must be overcome: the cell wall. Unlike mammalian cells, plant, fungal, and nearly all bacterial cells contain this complex mixture of carbohydrates and proteins that provides protection and support. The cell wall is a significant barrier to the delivery of molecules, and chemical-based gene delivery methods such as liposomes and lipid-based and polymeric nanoparticles are inefficient in penetrating the cell wall.

Our group has described an AuNP-mediated method that utilized an 800 nm Ti:sapphire laser to deliver the fluorescent dye calcein and pDNA into the model yeast *Saccharomyces cerevisiae* with a 35 fs pulse rate.[15] This was the first work demonstrating photoporation in fungal cells. Solutions of 10–20 nm AuNPs, cells, and either calcein or pDNA were exposed to laser pulses and successful delivery of calcein (<60%) and pDNA was achieved. Delivered plasmids included a plasmid tagged with BOBO-3 iodide, a blue fluorescent label (30% delivery), or a plasmid coding for mitochondrially expressed GFP with a positive selection marker LEU2 that enabled the successfully transformed cells to grow in leucine drop-out media (Fig. 3A). Due to the transient nature of the pores, delivery was achieved with a minor loss of viability. Ultimately, this demonstrates the potential of photoporation to successfully deliver nucleic acid
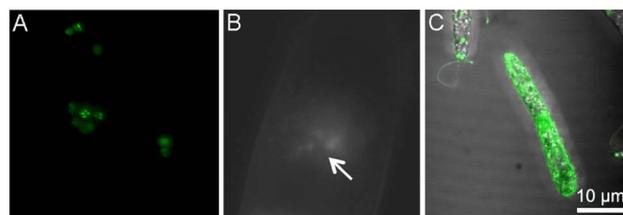


Fig. 3 (A) Mitochondrial EFGP expression in *S. cerevisiae* after AuNP-mediated photoporation. (B) Direct photoporation of propidium iodide into tobacco BY-2 cells. The arrow indicates where the laser was focused on the cell surface for irradiation. (C) Direct photoporation of a fluorescent aptamer into *E. gracilis*. All images were adapted with permission from ref. 15, 56, and 58, respectively.

therapies; however, further optimization and application in a clinically relevant fungal model are ongoing endeavors.

Literature reports on the photoporation of bacterial cells or biofilms are scarce. Bacteria biofilms play a crucial role in the context of disease because they often exhibit increased resistance to antibiotics and the host's immune system.[54] One of the only reports available for the irradiation of biofilms features a nanosecond laser system, a distinct difference from other photoporation systems. Teirlinck *et al.* exposed biofilms of both Gram negative (*Burkholderia multivorans* and *Pseudomonas aeruginosa*) and Gram positive (*Staphylococcus aureus*) bacteria to 70 nm AuNPs and irradiated with a single 7 ns pulse of a 561 nm laser.[55] Following the pulse, biofilms were subjected to antibiotics for 24 h. Irradiated groups showed greater antibiotic susceptibility than non-irradiated samples. This suggests that expansion of this technology may be utilized to deliver antibacterial therapies, as opposed to solely increasing the susceptibility of pathogens to an external treatment.

Mitchell *et al.* were some of the first to describe delivery of molecules into plant cells *via* direct photoporation.[56] In 2013, the authors reported the characterization of the vapor bubbles formed during direct photoporation and successful delivery of propidium iodide (PI) and fluorescently labeled dextrans using an 800 nm Ti:sapphire laser with a 140 fs pulse duration. Cells irradiated with PI showed both no lasting membrane damage and a permanent increase in cytosolic fluorescence, even minutes after photoporation (Fig. 3B). This is one of the only studies to report on the impact of beam type (Gaussian *vs.* Bessel). Additionally, while the authors state that a cargo size limit of 40–70 kDa may exist, other groups have since been able to deliver significantly larger molecules. Rukmana *et al.* also described direct photoporation in BY-2 cells using a similar 800 nm Ti:sapphire laser. A single 150 fs pulse was focused through an 100× objective of an Olympus scanning confocal microscope to deliver molecules of 2 MDa dextran using a single laser pulse.[57] However, this treatment was preceded by partial enzymatic degradation of two major cell wall components. While successful delivery of large cargoes is a significant addition to the literature, this study lacks an in-depth understanding of post-irradiation effects such as viability and proliferation. Both studies documented the transient effects of laser irradiation on cell wall morphology and agree that photoporation only minorly impacts viability.

Maeno *et al.* delivered a fluorescently labeled peptide aptamer using an 800 nm Ti:sapphire laser with a 100 fs pulse duration into *Euglena gracilis*, a microalgae.[58] This aptamer binds to paramylon produced by *E. gracilis* during photosynthesis, and cells were individually photoporated, allowing for spatially patterned delivery (Fig. 3C). While the authors claim that this method holds promise for microalgae-based metabolic engineering, much more work remains on exploring potential impacts on the metabolic processes, viability, and other bio-effects of photoporation in protists.[58]

# 4 Potential experimental setups for photoporation

One aspect that truly stands out in the current literature surrounding photoporation is the variety of experimental setups between groups. While this flexibility is one of the exciting things about photoporation systems, it also creates difficulties when attempting to directly compare data or discuss homogenization of the technique. As mentioned previously, setups consist of a complex network of experimental variables stemming from both the sample being irradiated and the instrumentation used for both irradiation and analysis. Samples generally consist of cells, which may incredibly delicate (like many primary lines) or resilient, such as non-mammalian cells. Additionally, both nanomaterials and cargo also vary widely in several aspects such as chemical composition, size, stability, concentration, and more (Fig. 4A). When considering instrumentation, decisions must be carefully made about cell containment (suspension *vs.* adherent, static *vs.* flow cell, *etc.*), laser specifics (laser type, wavelength, power, *etc.*), and an appropriate analysis method for the cargo (Fig. 4B).

A majority of photoporation systems utilize an inverted scanning microscope system that slowly scans a laser across a sample of adherent cells either contained in a plate or mounted on a slide, as depicted in Fig. 1A, but may also be a bench top apparatus that more complex optics equipment may be added to (mirrors, frequency doublers, *etc.*). The experimental setup for direct photoporation also generally involves cells that are placed on the stage of a scanning microscope.[3] These microscopes, such as confocal microscopes, are equipped with an appropriate laser which is focused through a lens, such as a microscope objective, and is systematically scanned across the specimen in a grid-like pattern. Samples are irradiated through a microscope objective at a set scanning speed, allowing for a specific amount of energy to be delivered to each cell in a given time frame. While this setup is simple, largely accessible in a variety of lab settings, and can be used for direct or indirect photoporation, it limits the lasers available for use and restricts the sample type to stationary or adherent cells. Additionally, sample processing times are high as each well or slide must be individually scanned. However, the duality of having a microscope attached allows for efficient sample imaging, even during irradiation, as demonstrated in Fig. 1B.

Experimental setups that utilize cells in solution are less common. Lukianova-Hleb and coworkers irradiated suspensions of HN31, NOM9, and peripheral blood mononuclear cells that had been exposed to AuNPs with a single 70 ps pulse of a 532 nm PL-2250 Nd:YAG laser as they passed through a clear micro-flow
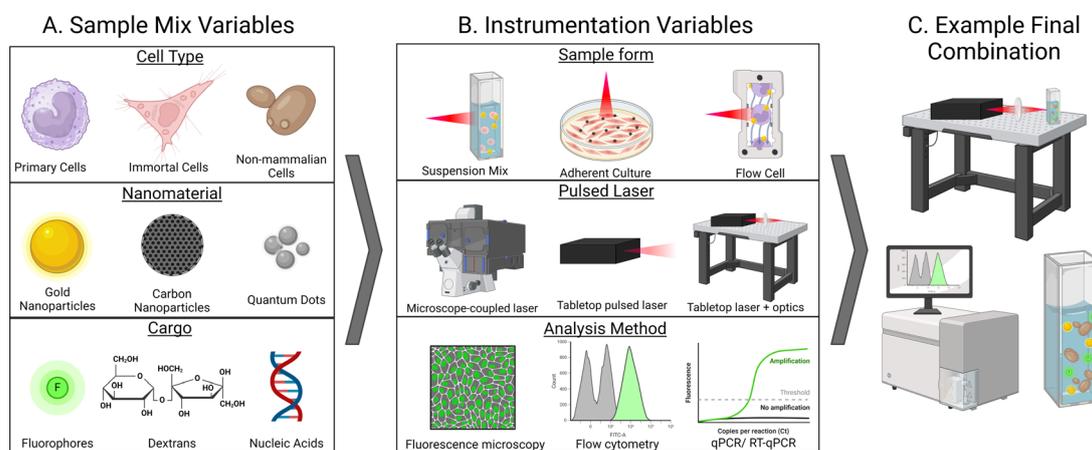


**Fig. 4** Schematic depicting examples of the complex network of variables that may be combined in an experimental set up. (A) The irradiated solution combines cells, nanoparticles, and cargo. Cell selection may be made based on how resilient the cells may be, or the research interest of the overall study. Nanomaterials, as discussed previously, have unique characteristics that may be desirable for delivering certain cargoes. Selection of the cargo has larger impacts, as this will also limit what types of analysis will be suitable. (B) Instrumentation possibilities include cell containment, the type of laser being used, and how the sample will be analyzed post-irradiation. Various laser setups may be used, including microscope-coupled lasers (often confocal systems), simple bench-top apparatuses, or more sensitive systems utilizing complex optics. The method in which the irradiation solution is exposed to the laser often changes depending on the laser. For example, a cell culture dish is more suitable for a microscope-coupled system than a flow cell system. Analysis methods often vary depending on the delivered molecule (*e.g.*, dye, pDNA, siRNA, *etc.*). Additionally, many reports are not consistent with reported data, such as viability reports or non-laser controls. This category largely defines how complex and potentially reproducible a setup is. (C) The final combined setup is a somewhat unique system, which presents the trade-off of being customized to the specific aim of the experiment while potentially being difficult to replicate by other groups. Created using https://BioRender.com.

cuvette (Fig. 4B, top).[32] Simple bench-top lasers such as this are generally commercially available but require some specialized equipment, such as a stabilizing air table and common optics equipment. Similar studies, such as by Schomaker *et al.* who delivered siRNA into CT1258 and ZMTH3 cells required a laser system equipped with more complex optics equipment, such as frequency doublers, beam splitters, and other optics (Fig. 4B, middle).[59] Additionally, this flow cell system allowed for the spatially precise generation of plasmonic nanobubbles resulting from in-resonance effects between the AuNPs and laser. In several studies, the Prausnitz group also photoporated suspensions of DU145 in the presence of CB nanoparticles using a bench top Nd:YAG 1064 nm laser with 5–9 ns pulses.[38,60,61] As discussed above, our group irradiated solutions of CHO and *Saccharomyces cerevisiae*, pDNA or calcein, and AuNPs suspended in a quartz cuvette using a 35 fs pulse 800 nm Ti:sapphire laser.[15] This setup required periodic solution mixing to ensure all cells were exposed to the laser path, although this could be automated in future studies. Furthermore, this type of cell suspension makes post-irradiation analysis by flow cytometry or time-dependent methods such as qPCR simple as cells do not need to be removed from a substrate prior to analysis. While other studies explore the photoporation of cells grown in suspension, they are generally allowed to settle upon a surface prior to photoporation with a scanning-type setup, as described in the previous paragraph and shown in Fig. 4B, top. For example, Liu *et al.* demonstrated that surface-modified graphene-based nanoparticles outperformed non-modified graphene QDs in both adherent HeLa and Jurkat (human T cell leukemia cells), but the suspension cells were allowed to settle upon a matrix prior to irradiation with one to two 7 ns pulse(s) of a Opolette HE 355 LD tuned to 561 nm.[62]

The exact experimental setup may be a limiting factor for the availability and user-friendliness of this technique. While scanning microscopes remain a prevalent laboratory tool, the potential of femtosecond lasers, despite facing cost-related constraints ($0.5 M) and stringent safety protocols, presents an exciting opportunity. Furthermore, this method will allow for high-throughput photoporation of thousands of cells. The variability in experimental setup parameters – such as laser wavelength, pulse speed, laser source, and physical arrangement (inverted *vs.* tabletop) – presents both advantages and challenges in the advancement of photoporation methodologies. While this variability allows each study to optimize parameters for individual experiments, it results in a lack of standardized cohesion across systems as the possible combination of experimental setups is vast (Fig. 4C). Consequently, this hampers the reproducibility of experiments between different research groups and adds complexity to the transition of a more comprehensive 'photoporation practice' into a pre-clinical setting, a topic we will explore in the subsequent discussion.

# 5 Clinical potential of photoporation

Electroporation (EP) is currently the only physical method to have been tested in clinical trials.[63–65] Mpendo *et al.* explored the tolerability of a multi-dose, multi-antigenic HIV DNA vaccine delivered

through intramuscular (IM) injection coupled with electroporation (IM/EP). The vaccine is first administered intramuscularly, followed by exposure of the injection site to EP pulses.[65,66] IM/EP vaccines have previously shown to increase immunogenicity to HIV-1 DNA vaccines compared to standard intramuscular injections.[67] Participants in the three-injection study largely considered the pain levels of the electrical stimulation as "none", "light", or "uncomfortable" for all three injections, while >~10% of participants reported "intense", "severe", or "very severe" pain up to 30 min after any of the injections.[65] However, a study performed by Trimble *et al.* focused on delivering an IM/EP vaccine against different HPVs found that ~91% of participants reported pain as a symptom.[68] While only 2 of 125 participants in the injection group discontinued out of pain, ~76% of participants reported grade 2–3 adverse events, which constitute moderate to severe but not life-threatening unwanted side effects, according to the Common Terminology Criteria for Adverse Events.[68]

While IM/EP DNA vaccines have shown increased immunogenicity compared to non-EP vaccines, this technique is painful and still requires a standard injection of a therapeutic agent, such as DNA.[65,66,69,70] Additionally, the lack of understanding on the exact biophysical mechanisms of how EP promotes delivery and conflicting reports of potential adverse reactions present a large barrier to the continued research and development of other physical delivery methods for clinical applications.

Different from chemical-based delivery methods in which nanoparticles can be introduced using different administration routes (*i.e.*, intravenous or intramuscular injections, intranasal sprays, *etc.*) the potential of laser-based therapies would be confined mostly to topical delivery. A femtosecond laser will penetrate <1 cm into the skin, making it ideal for dermatology or topical conditions such as infections or skin cancer.[71] Thus, one of the most realistic clinical translations of photoporation is the treatment of topical skin infections or conditions. As previously discussed, successful delivery into both bacterial biofilms and fungal cells has been achieved.[15,55] Both of these commonly infect the skin at a superficial level. Additionally, skin cancers or other conditions may benefit from topical drug and nucleic acid delivery as a treatment method.

An obstacle in the clinical translation of laser-assisted photoporation lies in the limited penetration of ultrashort laser pulses into human tissues, compounded by the molecular complexity of the targeted cells. Nonetheless, femtosecond pulses of light in the near-infrared range, typically around 800 nm (1 W cm$^{-2}$), can penetrate depths of 0.3 mm to 1 cm without damaging tissue integrity. This makes them particularly well-suited for potential targeting of topical infections or carcinomas associated with the skin, nails, hair, oral cavity, esophagus, or lower female reproductive tract. Specifically, the ability of laser-based photoporation to deliver molecules into fungal and bacterial cells could open avenues for fungicide and bactericide treatments against cutaneous and mucosal infections. In a clinical context, this approach could potentially involve the application of a topical aqueous nanoparticle solution to the affected area, followed by exposure to ultra-fast laser pulses (Fig. 5). However, it remains challenging to treat conditions affecting deeper internal organs or tumors.
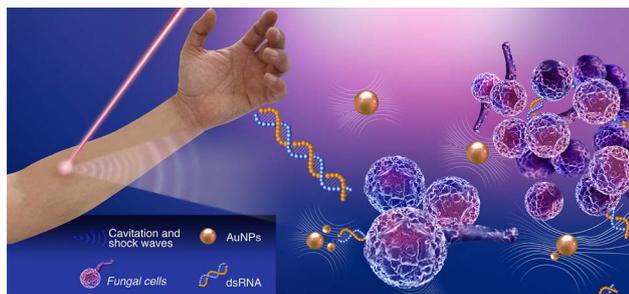
**Fig. 5** Schematic showing a potential setup of a clinical application of photoporation to deliver therapeutic nucleic acids to treat a topical fungal infection.

*Ex vivo* gene therapy, such as delivering CRISPR/Cas9 into stem cells, presents another avenue for exploration. While challenging due to the large components being involved, optimizing a nanoparticle solution to deliver these components could streamline the process. This therapy is particularly challenging due to the multiple, large components that need to be delivered. Potentially, a mixture of Cas9-mRNA and the correct guide RNA could be mixed in solution and delivered to stem cells. Additionally, direct delivery of the Cas9 riboprotein may be possible due to the pores in the membrane allowing for the entry of larger cargoes. Many nanoparticle-based systems have been developed to deliver one or more of these components; however, they face similar challenges mentioned earlier about chemical-based delivery systems.[72]

While photoporation has not yet advanced to the stage of clinical or pre-clinical trials, analogous therapies are already in development, setting the groundwork for the potential application of this technology.[71] For example, exploration of in-resonance effects has led to the development of a new therapeutic technique called plasmonic photothermal therapy (PPTT). In PPTT, AuNPs are intravenously delivered to cancerous cells and exposed to near-infrared (NIR) light. This method utilizes in-resonance nanoparticles that are delivered *via* IV and accumulate in a tumor site due to the enhanced permeability and retention effect (EPR) caused by the leaky vasculature surrounding tumors. The AuNPs are then activated with the NIR light, triggering the SPR effect that releases heat into the targeted tissue or tumor.[71] Versions of this therapy created by AuroLase have been explored in animal clinical trials for the treatment of spontaneous tumors in dogs and cats and is currently in the early stages of human clinical trials (**https://ClinicalTrials.gov** identifier: NCT02680535).[71] This therapy shows that AuNPs have promise as a therapeutic agent and parallels photoporation in how the AuNPs are energetically activated. This is encouraging for advancing photoporation from *in vitro* studies to *in vivo* experiments and eventually into pre-clinical and clinical trials.

## 6  Conclusions

Ultra-fast laser-assisted photoporation has emerged as an exciting technique for efficiently delivering membrane-impermeable molecules into various cells, including fungal, plant, and bacterial cells, as well as bacterial biofilms.[15,16,55] The potential application of photoporation in clinical drug delivery, particularly for local and topical treatments also holds significant promise. For instance, the treatment of topical dermatological conditions like fungal infections stands as a prime candidate for photoporation-based therapy. The unique mechanisms underlying molecule delivery into cells, such as laser-induced breakdown and cavitation, suggest a lower risk of systemic toxicity compared to conventional topical or systemic drug administration routes. Additionally, the capability to deliver target-specific molecules, such as RNAs, presents an exciting development for expanding therapeutic treatments.

Despite numerous successful photoporation systems for *in vitro* delivery, there is an astonishing lack of *in vivo* data. Pre-clinical studies in animal models are imperative to assess potential bioeffects arising from laser irradiation, such as immunotoxicity, generation of reactive species, genotoxicity, and cargo damage. Moreover, systematic optimization of nanoparticle and laser parameters specific to each experimental setup is scarcely documented.

Several challenges must be addressed to facilitate the clinical application of photoporation. For instance, understanding the fundamental mechanisms of laser-induced membrane perturbation, both in the presence and absence of nanoparticles, is vital for enhancing control and prediction of the influx of molecules varying in size and charge into the cytosol, as well as for determining the duration of membrane openings. While current photoporation methods predominantly focus on plasmid DNA (pDNA) delivery, it is crucial to explore other therapeutic nucleic acids, such as mRNA, dsRNA, or siRNA, while also investigating potential genotoxic effects on irradiated cells.

Overall, the advancement of photoporation has come a long way, but many avenues remain to be explored. This method relies on a complex set of variables, including the laser type, laser fluence, irradiation time, presence of nanoparticles, parameters of those nanoparticles (shape, size, concentration, *etc.*), type of cargo, what type of cell is being targeted, and many others. As this is still a new technique, there is additionally a lack of *in vivo* data. Despite all of this, the current *in vitro* data show that this method is capable of effectively delivering a range of molecules into fungal, bacterial, plant, and mammalian cells. Pre-clinical and clinical studies using a similar technique, photothermal therapy, have shown promising results, suggesting that the clinical translation of photoporation to deliver drugs or therapeutic nucleic acids to treat topical infections is hopeful.

## Data availability

No primary research results, software, or code has been included, and no new data were generated or analyzed as part of this review.

## Conflicts of interest

There are no conflicts to declare.

# Notes and references

1 T. K. Kim and J. H. Eberwine, *Anal. Bioanal. Chem.*, 2010, **397**, 3173–3178.

2 N. Nayerossadat, P. Ali and T. Maedeh, *Adv. Biomed. Res.*, 2012, **1**, 27.

3 M. Antkowiak, M. L. Torres-Mapa, F. Gunn-Moore and K. Dholakia, *J. Biophot.*, 2010, **3**, 696–705.

4 N. Linz, S. Freidank, X. X. Liang and A. Vogel, *Phys. Rev. B*, 2016, **94**, 024113.

5 P. Chakravarty, W. Qian, M. A. El-Sayed and M. R. Prausnitz, *Nat. Nanotechnol.*, 2010, **5**, 607–611.

6 P. Wang, L. Zhang, W. Zheng, L. Cong, Z. Guo, Y. Xie, L. Wang, R. Tang, Q. Feng, Y. Hamada, K. Gonda, Z. Hu, X. Wu and X. Jiang, *Angew. Chem., Int. Ed.*, 2018, **57**, 1491–1496.

7 D. Heinemann, S. Kalies, M. Schomaker, W. Ertmer, H. M. Escobar, H. Meyer and T. Ripken, *Nanotechnology*, 2014, **25**, 245101.

8 S. Batabyal, S. Kim, W. Wright and S. Mohanty, *J. Biophot.*, 2021, **14**, e202000234.

9 L. Paterson, B. Agate, M. Comrie, R. Ferguson, T. K. Lake, J. E. Morris, A. E. Carruthers, C. T. Brown, W. Sibbett, P. E. Bryant, F. Gunn-Moore, A. C. Riches and K. Dholakia, *Opt. Express*, 2005, **13**, 595–600.

10 R. Xiong, S. K. Samal, J. Demeester, A. G. Skirtach, S. C. De Smedt and K. Braeckmans, *Adv. Phys.: X*, 2016, **1**(4), 596–620.

11 G. Sinibaldi, A. Occhicone, F. Alves Pereira, D. Caprini, L. Marino, F. Michelotti and C. M. Casciola, *Phys. Fluids*, 2019, **31**, 103302.

12 Ã. Boulais, R. Lachaine and M. Meunier, *Nano Lett.*, 2012, **12**, 4763–4769.

13 R. L. Gieseking, *Mater. Horiz.*, 2022, **9**, 25–42.

14 N. Saklayen, S. Kalies, M. Madrid, V. Nuzzo, M. Huber, W. Shen, J. Sinanan-Singh, D. Heinemann, A. Heisterkamp and E. Mazur, *Biomed. Opt. Express*, 2017, **8**, 4756.

15 E. McGraw, R. R. Dissanayaka, J. J. Vaughan, N. Kunte, G. Mills, G. G. G. Laurent and L. A. Avila, *ACS Appl. Bio Mater.*, 2020, **3**, 6167–6176.

16 S. Hosseinpour and L. J. Walsh, *J. Biophotonics*, 2021, **14**(1), e202000295.

17 V. Amendola, R. Pilot, M. Frasconi, O. M. Maragò and M. A. Iatì, *J. Phys.: Condens.Matter*, 2017, **29**, 203002.

18 T. S. Santra, S. Kar, T. C. Chen, C. W. Chen, J. Borana, M. C. Lee and F. G. Tseng, *Nanoscale*, 2020, **12**, 12057–12067.

19 R. Xiong, K. Raemdonck, K. Peynshaert, I. Lentacker, I. De Cock, J. Demeester, S. C. De Smedt, A. G. Skirtach and K. Braeckmans, *ACS Nano*, 2014, **8**, 6288–6296.

20 E. Y. Lukianova-Hleb, E. Y. Hanna, J. H. Hafner and D. O. Lapotko, *Nanotechnology*, 2010, **21**, 085102.

21 A. Vogel, J. Noack, G. Hüttman and G. Paltauf, *Appl. Phys. B*, 2005, **81**, 1015–1047.

22 X. Huang and M. A. El-Sayed, *J. Adv. Res.*, 2010, **1**(1), 13–28.

23 T. Pylaev, E. Avdeeva and N. Khlebtsov, *J. Innovative Opt. Health Sci.*, 2021, **14**, 2021–2035.

24 L. F. Leopold, I. S. Tódor, Z. Diaconeasa, D. Rugină, A. Ştefancu, N. Leopold and C. Coman, *Colloids Surf., A*, 2017, **532**, 70–76.

25 C. M. Pitsillides, E. K. Joe, X. Wei, R. R. Anderson and C. P. Lin, *Biophys. J.*, 2003, **84**, 4023–4032.

26 R. Xiong, F. Sauvage, J. C. Fraire, C. Huang, S. C. De Smedt and K. Braeckmans, *Acc. Chem. Res.*, 2023, **56**, 631–643.

27 Ã. Boulais, R. Lachaine and M. Meunier, *J. Phys. Chem. C*, 2013, **117**, 9386–9396.

28 R. Xiong, R. X. Xu, C. Huang, S. De Smedt and K. Braeckmans, *Chem. Soc. Rev.*, 2021, **50**, 5746–5776.

29 J. M. Teulon, C. Godon, L. Chantalat, C. Moriscot, J. Cambedouzou, M. Odorico, J. Ravaux, R. Podor, A. Gerdil, A. Habert, N. Herlin-Boime, S. W. W. Chen and J. L. Pellequer, *Nanomaterials*, 2019, **9**, 18.

30 A. Sukhanova, S. Bozrova, P. Sokolov, M. Berestovoy, A. Karaulov and I. Nabiev, *Nanoscale Res. Lett.*, 2018, **13**, 44.

31 R. Mendes, P. Pedrosa, J. C. Lima, A. R. Fernandes and P. V. Baptista, *Sci. Rep.*, 2017, **7**, 1–9.

32 E. Y. Lukianova-Hleb, D. S. Wagner, M. K. Brenner and D. O. Lapotko, *Biomaterials*, 2012, **33**, 5441–5450.

33 E. Y. Lukianova-Hleb, M. B. Mutonga and D. O. Lapotko, *ACS Nano*, 2012, **6**, 10973–10981.

34 C. Yao, R. Rahmanzadeh, E. Endl, Z. Zhang, J. Gerdes and G. Hüttmann, *J. Biomed. Opt.*, 2005, **10**, 064012.

35 J. Liu, R. Xiong, T. Brans, S. Lippens, E. Parthoens, F. C. Zanacchi, R. Magrassi, S. K. Singh, S. Kurungot, S. Szunerits, H. Bové, M. Ameloot, J. C. Fraire, E. Teirlinck, S. K. Samal, R. D. Rycke, G. Houthaeve, S. C. De Smedt, R. Boukherroub and K. Braeckmans, *Light: Sci. Appl.*, 2018, **7**, 1–10.

36 J. Wang, A. Harizaj, Y. Wu, X. Jiang, T. Brans, J. C. Fraire, J. M. Morales, S. C. De Smedt, Z. Tang, R. Xiong and K. Braeckmans, *Nanoscale*, 2021, **13**, 17049–17056.

37 S. Y. Holguin, M. D. Gray, P. Joseph, N. N. Thadhani and M. R. Prausnitz, *Adv. Healthcare Mater.*, 2018, **7**, 1701007.

38 A. Sengupta, S. C. Kelly, N. Dwivedi, N. Thadhani and M. R. Prausnitz, *ACS Nano*, 2014, **8**, 2889–2899.

39 G. Hong, S. Diao, A. L. Antaris and H. Dai, *Chem. Rev.*, 2015, **115**, 10816–10906.

40 R. Xiong, D. Hua, J. Van Hoeck, D. Berdecka, L. Léger, S. De Munter, J. C. Fraire, L. Raes, A. Harizaj, F. Sauvage, G. Goetgeluk, M. Pille, J. Aalders, J. Belza, T. Van Acker, E. Bolea-Fernandez, T. Si, F. Vanhaecke, W. H. De Vos, B. Vandekerckhove, J. van Hengel, K. Raemdonck, C. Huang, S. C. De Smedt and K. Braeckmans, *Nat. Nanotechnol.*, 2021, **16**(11), 1281–1291.

41 L. Mohan, S. Kar, R. Hattori, M. Ishii-Teshima, P. Bera, S. Roy, T. S. Santra, T. Shibata and M. Nagai, *Appl. Surf. Sci.*, 2021, **543**, 148815.

42 Y. Q. He, S. P. Liu, L. Kong and Z. F. Liu, *Spectrochim. Acta, Part A*, 2005, **61**, 2861–2866.

43 Y. C. Wu, T. H. Wu, D. L. Clemens, B. Y. Lee, X. Wen, M. A. Horwitz, M. A. Teitell and P. Y. Chiou, *Nat. Methods*, 2015, **12**, 439–444.

44 G. González-Rubio, A. Guerrero-Martínez and L. M. Liz-Marzán, *Acc. Chem. Res.*, 2016, **49**, 678–686.

45 S. Bhandari, B. Hao, K. Waters, C. H. Lee, J. C. Idrobo, D. Zhang, R. Pandey and Y. K. Yap, *ACS Nano*, 2019, **13**, 4347–4353.

46 A. M. Wagner, J. M. Knipe, G. Orive and N. A. Peppas, *Int. J. Nanomed.*, 2019, **17**, 1951–1970.

47 M. J. O'Connell, S. H. Bachilo, C. B. Huffman, V. C. Moore, M. S. Strano, E. H. Haroz, K. L. Rialon, P. J. Boul, W. H. Noon, C. Kittrell, J. Ma, R. H. Hauge, R. B. Weisman and R. E. Smalley, *Science*, 2002, **297**, 593–596.

48 T. B. Napotnik, T. Polajžer and D. Miklavčič, *Bioelectrochemistry*, 2021, **141**, 107871.

49 A. J. Jimenez and F. Perez, *Curr. Opin. Cell Biol.*, 2017, **47**, 99–107.

50 A. J. Jimenez and F. Perez, *Semin. Cell Dev. Biol.*, 2015, **45**, 2–9.

51 A. Horn and J. K. Jaiswal, *Cell. Mol. Life Sci.*, 2018, **75**(20), 3751–3770.

52 R. Palankar, B. E. Pinchasik, B. N. Khlebtsov, T. A. Kolesnikova, H. Möhwald, M. Winterhalter and A. G. Skirtach, *Nano Lett.*, 2014, **14**, 4273–4279.

53 S. Kalies, D. Heinemann, M. Schomaker, H. M. Escobar, A. Heisterkamp, T. Ripken and H. Meyer, *J. Biophot.*, 2014, **7**, 825–833.

54 L. Hall-Stoodley, J. W. Costerton and P. Stoodley, *Nat. Rev. Microbiol.*, 2004, **2**(2), 95–108.

55 E. Teirlinck, R. Xiong, T. Brans, K. Forier, J. Fraire, H. Van Acker, N. Matthijs, R. De Rycke, S. C. De Smedt, T. Coenye and K. Braeckmans, *Nat. Commun.*, 2018, **9**, 4518.

56 C. A. Mitchell, S. Kalies, T. Cizmár, A. Heisterkamp, L. Torrance, A. G. Roberts, F. J. Gunn-Moore and K. Dholakia, *PLoS One*, 2013, **8**, e79235.

57 T. I. Rukmana, G. Moran, R. Méallet-Renault, M. Ohtani, T. Demura, R. Yasukuni and Y. Hosokawa, *Sci. Rep.*, 2019, **9**, 1–9.

58 T. Maeno, T. Uzawa, I. Kono, K. Okano, T. Iino, K. Fukita, Y. Oshikawa, T. Ogawa, O. Iwata, T. Ito, K. Suzuki, K. Goda and Y. Hosokawa, *Sci. Rep.*, 2018, **8**, 1–9.

59 M. Schomaker, D. Heinemann, S. Kalies, S. Willenbrock, S. Wagner, I. Nolte, T. Ripken, H. M. Escobar, H. Meyer and A. Heisterkamp, *J. Nanobiotechnol.*, 2015, **13**, 1–15.

60 S. Y. Holguin, N. N. Thadhani and M. R. Prausnitz, *Nanomedicine*, 2018, **14**, 1667–1677.

61 S. Kumar, E. Lazau, C. Kim, N. N. Thadhani and M. R. Prausnitz, *Int. J. Nanomed.*, 2021, **16**, 3707–3724.

62 J. Liu, C. Li, T. Brans, A. Harizaj, S. Van de Steene, T. De Beer, S. De Smedt, S. Szunerits, R. Boukherroub, R. Xiong and K. Braeckmans, *Int. J. Mol. Sci.*, 2020, **21**, 1540.

63 N. Y. Sardesai and D. B. Weiner, *Curr. Opin. Immunol.*, 2011, **23**(3), 421–429.

64 L. Lambricht, A. Lopes, S. Kos, G. Sersa, V. Préat and G. Vandermeulen, *Expert Opin. Drug Delivery*, 2016, **13**(2), 295–310.

65 J. Mpendo, G. Mutua, A. Nanvubya, O. Anzala, J. Nyombayire, E. Karita, L. Dally, D. Hannaman, M. Price, P. E. Fast, F. Priddy, H. C. Gelderblom and N. K. Hills, *PLoS One*, 2020, **15**, e0233151.

66 M. Wallace, B. Evans, S. Woods, R. Mogg, L. Zhang, A. C. Finnefrock, D. Rabussay, M. Fons, J. Mallee, D. Mehrotra, F. Schödel and L. Musey, *Mol. Ther.*, 2009, **17**, 922–928.

67 S. Vasan, A. Hurley, S. J. Schlesinger, D. Hannaman, D. F. Gardiner, D. P. Dugin, M. Boente-Carrera, R. Vittorino, M. Caskey, J. Andersen, Y. Huang, J. H. Cox, T. Tarragona-Fiol, D. K. Gill, H. Cheeseman, L. Clark, L. Dally, C. Smith, C. Schmidt, H. H. Park, J. T. Kopycinski, J. Gilmour, P. Fast, R. Bernard and D. D. Ho, *PLoS One*, 2011, **6**, e19252.

68 C. L. Trimble, M. P. Morrow, K. A. Kraynyak, X. Shen, M. Dallas, J. Yan, L. Edwards, R. L. Parker, L. Denny, M. Giffear, A. S. Brown, K. Marcozzi-Pierce, D. Shah, A. M. Slager, A. J. Sylvester, A. Khan, K. E. Broderick, R. J. Juba, T. A. Herring, J. Boyer, J. Lee, N. Y. Sardesai, D. B. Weiner and M. L. Bagarazzi, *Lancet*, 2015, **386**, 2078–2088.

69 E. N. Gary and D. B. Weiner, *Curr. Opin. Immunol.*, 2020, **65**, 21–27.

70 L. Low, A. Mander, K. McCann, D. Dearnaley, T. Tjelle, I. Mathiesen, F. Stevenson and C. H. Ottensmeier, *Hum. Gene Ther.*, 2009, **20**, 1269–1278.

71 M. R. Ali, Y. Wu and M. A. El-Sayed, *J. Phys. Chem. C*, 2019, **123**, 15375–15393.

72 L. Duan, K. Ouyang, X. Xu, L. Xu, C. Wen, X. Zhou, Z. Qin, Z. Xu, W. Sun and Y. Liang, *Front. Genet.*, 2021, **12**, 673286.